Microwave Mode Locking at *X* Band Using Solid-State Devices

LANCE A. GLASSER AND HERMANN A. HAUS, FELLOW, IEEE

Abstract—**A theory of mode locking in the microwave regime is presented. The use of solid-state microwave devices for this application is described. A system that has been built using an IMPATT diode as the gain element and a Schottky barrier diode in the role of a saturable absorber is analyzed. Passive, combined passive, and forced mode locking have been demonstrated experimentally. The system had a round-trip time of 25 or 50 ns. Pulse lengths between 4 and 15 ns were observed. Self-starting and stability requirements are investigated.**

I. Introduction

Although it is, at present, of particular importance to laser technology, mode locking was originally proposed and accomplished in the microwave regime by C. C. Cutler [1]. In 1955 he described a "regenerative pulse generator" that operates essentially in the same way as the system described here, as well as its cousins in the optical regime. Cutler's theory, however, predicted Gaussian pulses that were not observed in the experiments reported here.

The mode locking described here, in fact, is more closely related to the laser fast saturable absorber systems [2] now used in the optical regime than to Cutler's original version. The system described here and most of the laser systems contain reflection resonators, whereas Cutler's system is a ring resonator.

Mode locking is represented by a set of equations and any system satisfying these equations will work. A microwave mode locking system composed of solid-state devices can take many forms. In general, there will be four elements. One requirement is for a negative resistance element, such as an IMPATT, Gunn, BARITT, or TRAPATT diode, which acts in a fashion analogous to the laser in optical systems. A second requirement is for a nonlinear element whose loss goes down as the incident radiation increases. The rest of the elements are a transmission line or filter to provide delay and a cavity to provide bandwidth limiting.

The system that we shall analyze, and which has been tested experimentally, is shown in Fig. 1. The active element is an IMPATT diode in a cavity. A waveguide "delay line" connects it to a Schottky diode in a feedback circuit. The feedback circuit changes the bias current as a function of the average RF power. The time constant of the feedback circuit is such as to ensure self-starting of the mode-locked pulses and to prevent relaxation oscillations. We begin with a theoretical analysis of the function of the IMPATT diode and of the Schottky diode in Sections II and III.

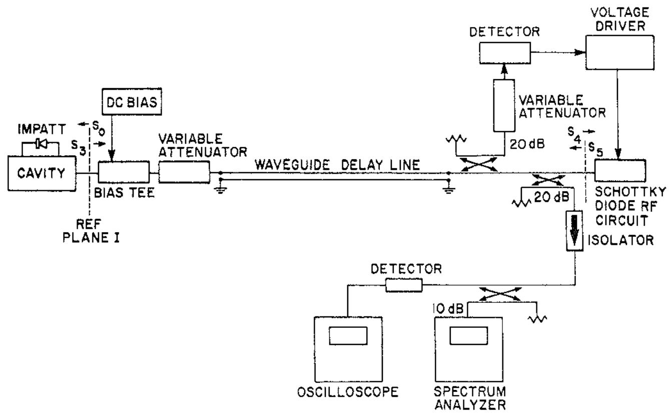

Fig. 1. Microwave mode-locking system.

In Section IV we combine the actions of these two diodes via the waveguide delay line and obtain a slight generalization of the laser mode-locking equation in that the Schottky diode provides not only a resistive but also a reactive saturation effect. The result is a secant hyperbolic pulse envelope as a function of time and a chirp of the mode-locked pulse. In Section V we study the self-starting conditions, and in Section VI the prevention of relaxation oscillations. Section VII presents the experimental results.

Saturable absorber mode locking at 10 GHz in a waveguide giving a 50-ns roundtrip time led to pulses varying in length between 15 to 5 ns with either one or two pulses per round-trip time. With a shortened system of 25 ns, round-trip time single pulses of 4 ns width were observed. Maximum pulse power of 10 mW was measured. No attempt was made to optimize the pulse power.

II. The Reflection Amplifier

The microwave amplifier circuit to the left of reference plane *I* in Fig. 1 may be modeled as shown in Fig. 2. The attenuator, placed between reference planes *I* and *J*, models the low-Q or frequency-independent loss of the amplifier. The series resonant circuit to the right of reference plane *J* models the frequency dependence and gain portions of the amplifier. This phenomenological model has the advantage that the attenuation Q, of the resonant circuit, the value of negative resistance R, may all be read off of an experimentally represented Smith chart plot of the amplifier.

Manuscript received February 4, 1977; revised June 29, 1977. This work was supported in part by the Joint Services Electronics Program under Contract DAAB07-76-C-1400.

The authors are with the Research Laboratory of Electronics and the Department of Electrical Engineering and Computer Science, Massachusetts Institute of Technology, Cambridge, MA 02139.

0018-9480/78/0200-0062$00.75 © 1978 IEEE

The amplifier is assumed to operate in its linear region, a good approximation for this system which uses a medium power IMPATT diode. If we were to optimize for power, we would have to include in the analysis the effects of amplifier nonlinearities.

The output of a mode-locked system gives pulses of high-frequency energy. The analysis will deal, therefore, with voltage and current envelopes rather than with their instantaneous values.

If the normalized impedance of the IMPATT diode is Z, then the reflection coefficient is given by

$$\Gamma = \frac{Z-1}{Z+1}. \tag{1}$$

In the time domain, $\Gamma(\omega)$ transforms into a differential operator. Suppose the voltage of the incident wave is given by $s_1(t)e^{j\omega_0 t}$, where $s_1(t)$ is a function with a bandwidth that is narrow compared with the carrier frequency ω_0. Then, in the time domain, the action of the reflection coefficient on $s_1(t)$, so as to produce a reflected wave $s_2(t)$, may be taken as the Fourier transform of a Taylor expansion of $\Gamma(\omega)$ around ω_0 to second order in $\omega - \omega_0$:

$$s_2(t) = \Gamma s_1(t) \tag{2}$$

where

$$\Gamma = \Gamma(\omega_0) - j\Gamma'(\omega)\bigg|_{\omega=\omega_0} \frac{\partial}{\partial t} - \frac{1}{2}\Gamma''(\omega)\bigg|_{\omega=\omega_0} \frac{\partial^2}{\partial t^2} \tag{3}$$

$$\Gamma' = 2Z'(Z+1)^{-2} \tag{4}$$

$$\Gamma'' = \frac{2Z''}{(Z+1)^2} - \frac{4(Z')^2}{(Z+1)^3}. \tag{5}$$

Introducing the parameters of the system to the right of reference plane J in Fig. 2, we may write

$$\Gamma(\omega_0) \equiv \Gamma_{IO} = \frac{R-1}{R+1} \tag{6}$$

$$-j\Gamma'(\omega)\bigg|_{\omega=\omega_0} = \frac{-4QR}{\omega_0(R+1)^2} \tag{7}$$

$$-\tfrac{1}{2}\Gamma''(\omega)\bigg|_{\omega=\omega_0} \cong \frac{-8Q^2R^2}{\omega_0^2(R+1)^3} \tag{8}$$

where we have defined

$$\omega_0^2 \equiv 1/LC \qquad Q \equiv -\frac{\omega_0 L}{R}. \tag{9}$$

Without loss of generality we shall assume that R, which is negative, is smaller in magnitude than unity so that $\Gamma_{IO} < -1$. Accordingly, we find that the operator (3) may be written

$$\Gamma = \Gamma_{IO}\left[1 - \frac{4QR}{\omega_0(R+1)^2\Gamma_{IO}}\frac{\partial}{\partial t} + \frac{8Q^2R^2}{\omega_0^2(R+1)^3(-\Gamma_{IO})}\frac{\partial^2}{\partial t^2}\right] \tag{10}$$

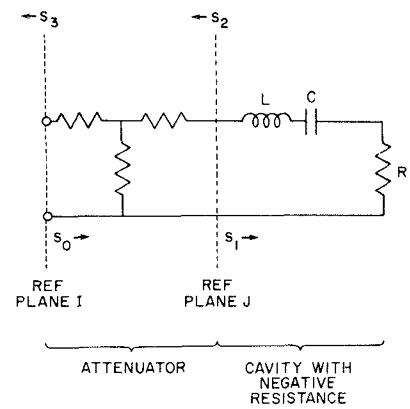

Fig. 2. Equivalent circuit of the reflection amplifier.

where the coefficient of $\partial/\partial t$ is negative and that of $\partial^2/\partial t^2$ is positive. Equation (2), in conjunction with (10), indicates that an incident "wave" $s_1(t)$ is transformed into $s_2(t)$ 1) by delay

$$\delta T = \frac{4QR}{\omega_0(R+1)^2\Gamma_{IO}}$$

2) with a spreading by the diffusion operator $\partial^2/\partial t^2$ multiplied by a positive coefficient, and 3) a multiplication by Γ_{IO} which causes gain and sign reversal, as behooves reflection of a voltage from a normalized impedance of magnitude less than unity.

Thus far we have defined the action of the circuit to the right of the reference plane J. Let $s(t)$ be normalized such that $s(t)^*s(t)$ is the power. Referring to Fig. 2, we may define the "gain" G_I so that

$$s_1(t) \equiv \sqrt{G_I}\, s_0(t). \tag{11}$$

$s_2(t)$ is related to $s_1(t)$ by (2) where Γ is an operator. Finally,

$$s_3(t) = \sqrt{G_I}\, s_2(t). \tag{12}$$

Combining, we obtain

$$s_3(t) = G_I\Gamma_{IO}\left[1 - \frac{4QR}{\omega_0\Gamma_{IO}(R+1)^2}\frac{\partial}{\partial t} + \frac{8Q^2R^2}{\omega_0^2(-\Gamma_{IO})(R+1)^3}\frac{\partial^2}{\partial t^2}\right]s_0(t). \tag{13}$$

Inside the brackets, the coefficient of $\partial/\partial t$ is negative, that of $\partial^2/\partial t^2$ is positive.

III. The Schottky Barrier Diode as a Fast Absorber

The Schottky barrier diode, a majority carrier device, is used as the nonlinear element because it is very fast. We believe that for this application p-i-n diodes are too slow. It is possible to operate the diode in either a reverse-biased varactor mode or in a forward-biased resistive mode. The latter was chosen because it permits loss modulation in a straightforward manner. At large forward biases the resistance of a Schottky diode becomes small and the capaci-

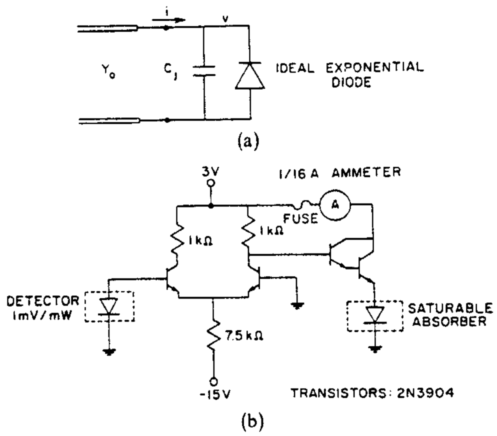

Fig. 3. Equivalent circuit of the Schottky diode termination and the feedback circuit.

tance becomes large. In this analysis we shall assume that the capacitance remains constant and ignore varactor and series resistance effects.

Fig. 3(a) shows a simple microwave model of the diode. C_j represents the junction and package capacitances. From Saleh [3], we have

$$i = 2I_{dc}\frac{v}{|v|}I_1(|\alpha v|) + j\omega_0 C_j v \tag{14}$$

where $I_1(x)$ is a modified Bessel function of the first kind,

$$I_{dc} \equiv I_0 \exp(\alpha V_{dc})$$

where

$$\alpha = q/kT \tag{15}$$

and the dc supply to the diode approximates a voltage source. The time derivatives of v, which would arise from an envelope expansion of the capacitive susceptance, are neglected in comparison with those caused by the reactive contribution of the cavity surrounding the IMPATT. Expanding equation (14), we get

$$i \approx 2I_{dc}\left(\frac{\alpha v}{2} + \frac{\alpha^3|v|^2 v}{16} + \cdots\right) + j\omega_0 C_j v. \tag{16}$$

For reasons that soon will become obvious, we invert this series. Let

$$v \equiv A_1 i + A_3|i|^2 i. \tag{17}$$

Solving, we obtain

$$A_1 = (\alpha I_{dc} + j\omega_0 C_j)^{-1} \equiv 2\eta \tag{18}$$

$$A_3 = -2\eta^2\alpha^3 I_{dc}|\eta|^2 \tag{19}$$

and for the normalized impedance Z_s of the Schottky diode

$$Z_s = (2\eta - 2\eta^2\alpha^3 I_{dc}|\eta i|^2)/Z_0. \tag{20}$$

It is desirable now to relate Z_s to the reflection coefficient of the Schottky barrier diode Γ and also to put $i(t)$ in terms of $s(t)$. For a transmission line,

$$2s(t) = \sqrt{Y_0}\,v(t) + \sqrt{Z_0}\,i(t) = [Z_s + 1]\sqrt{Z_0}\,i(t). \tag{21}$$

For a large forward bias, we have $Z_s \ll 1$; therefore, the current i is (approximately) proportional to the forward wave s:

$$i \approx 2\sqrt{Y_0}\,s. \tag{22}$$

Furthermore,

$$\Gamma \approx -(1 - 2Z_s). \tag{23}$$

From Fig. 1,

$$s_5(t) = \Gamma(t)s_4(t) \tag{24}$$

where Γ is obtained by combining (20)–(23).

$$\Gamma \approx -1 + 4Y_0\eta - (4Y_0)^2\eta^2\alpha^3 I_{dc}|\eta s_5|^2. \tag{25}$$

The physical interpretation of (25) is that a voltage pulse incident upon the diode and transformed via (24) will experience a linear loss $4Y_0\eta$ that is reduced by $(4Y_0)^2\eta^2\alpha^3 I_{dc}|\eta s_5|^2$ when the signal increases and then experiences a reversal because the termination has a normalized impedance of magnitude smaller than unity. The reduction of loss at high signal levels is required for mode locking, in order to compensate for the "diffusion in time" caused by the bandwidth-limited gain.

If the system is to be self-starting, a slow relaxation time constant must be associated with one of the elements in the system. This time constant may be associated with the IMPATT diode or the Schottky diode, or can be introduced by a separate component such as a p-i-n diode or ferrite limiter. In the present case the slow time constant was incorporated into the Schottky diode bias drive by detecting the power in the transmission line with the use of a directional coupler–detector scheme in conjunction with the voltage driver illustrated in Fig. 3(b).

The remaining element in this system is a waveguide delay line. An X-band standard rectangular waveguide was used in the fundamental mode. We have (see Fig. 1)

$$s_0'(t) = \sqrt{G_L}\,s_5\left(t - \frac{T_R}{2}\right) \tag{26}$$

and

$$s_4(t) = \sqrt{G_L}\,s_3\left(t - \frac{T_R}{2}\right) \tag{27}$$

where $s_0'(t)$ is the wave incident upon reference plane I after one transit. The dispersion associated with the waveguide is ignored.

IV. The Mode-Locking Equation and Its Solution

The closure condition necessitates that after one transit, $s_0(t)$, i.e., $s_0'(t)$, be a reproduction of $s_0(t)$, except for a possible time delay different from T_R and a possible phase-shift factor $e^{j\psi}$ indicating that the carrier $\exp j\omega_0 t$ has been changed in phase. Thus, dropping the subscript 0 on s,

$$s(t - \text{time delay})e^{j\psi} \cong G\left\{1 + \left(\frac{-4QR}{\omega_0(R+1)^2\Gamma_{IO}}\right)\frac{\partial}{\partial t} + \left(\frac{-8Q^2R^2}{\omega_0^2(R+1)^3\Gamma_{IO}}\right)\frac{\partial^2}{\partial t^2} + (-4\eta Y_0) + (4Y_0\eta\alpha)^2\alpha I_{dc}|\eta s|^2\right\}s(t - T_R). \tag{28}$$

Here we have defined $G \equiv G_I G_L(-\Gamma_{IO})$. G is the total linear nondispersive part of the gain. Since $\Gamma_{IO} < -1$, G is > 0. The term on the right-hand side of (28) multiplying $s(t)$ represents the action on the pulse by the linear loss, the nondispersive part of the gain, and the Schottky diode in its linear regime (i.e., the $|s|^2$ contribution is negligible). If mode-locked pulses separated by long time intervals are to exist, no gain should be experienced by a (noise) perturbation in that interval, otherwise the pulse solution would be unstable. Therefore, we require

$$1 - G + 4\,\mathrm{Re}\,(\eta) Y_0 G > 0. \qquad (29)$$

Since there is no net gain in the time interval between pulses when the Schottky diode is unsaturable, the system would not be self-starting if there were no possibility of the Schottky diode reducing its loss in the complete absence of a signal. This loss reduction in the absence of a signal is accomplished by the feedback circuit shown in Fig. 1 which has a time constant slow compared with the pulse round-trip time.

The function $s(t - \text{time delay})e^{j\psi}$ may be expanded to first order on the delay time deviation from T_R, δT, and phase angle ψ, so that

$$s(t - T_R - \delta T)e^{j\psi} \approx s(t - T_R) - \delta T \frac{\partial s(t - T_R)}{\partial t} + j\psi s(t - T_R). \qquad (30)$$

When (30) is introduced in (28), and steady-state pulse solutions are sought, no first-order time derivatives can appear in the equation because it can be shown that an isolated pulse solution is impossible in this case. This requirement determines the delay time δT. There remains the equation

$$\frac{\partial^2 s}{\partial t^2} + \frac{\omega_0^2 (R+1)^3 (-\Gamma_{IO})}{8Q^2R^2}(G - 1 - 4\eta Y_0 G - j\psi)s + \frac{\omega_0^2 (R+1)^3(-\Gamma_{IO})}{2Q^2R^2}(2Y_0\eta\alpha)^2 \alpha I_{\mathrm{dc}} |\eta s|^2 s = 0. \qquad (31)$$

In this equation ψ, the phase change after one transit, is an adjustable parameter. Hence, in solving (31) we must look for pulselike solutions, under the constraint (29), with ψ adjustable, and take into account that the coefficient of $|s|^2 s$ is positive. This equation is slightly different from the standard mode-locking equation solved previously [2] because η is complex. It takes the form

$$\frac{\partial^2}{\partial t^2} s + \hat{A}s + \hat{B}|s|^2 s = 0 \qquad (32)$$

where $\hat{A}$ and $\hat{B}$ are complex.

$$\hat{A} = \frac{1}{4}\left[\frac{-\omega_0^2(R+1)^3(-\Gamma_{IO})}{2Q^2R^2}\right](G - 1 - 4\eta Y_0 G - j\psi) \qquad (33)$$

$$\hat{B} = \left[\frac{\omega_0^2(R+1)^3(-\Gamma_{IO})}{2Q^2R^2}\right](2Y_0\eta\alpha)^2 \alpha I_{\mathrm{dc}}|\eta|^2. \qquad (34)$$

Note that the term in brackets is positive; therefore, $\mathrm{Re}\,\hat{A} < 0$ according to (29). A solution of (32) is [4]

$$s(t) = \frac{v_0}{\cosh(t/\tau_p)} \exp\left(j\frac{a}{\tau_p}\int^t \tanh(t/\tau_p)\,dt\right) \qquad (35)$$

where

$$\frac{1}{(v_0\tau_p)^2}(2 - a^2 - 3ja) = \hat{B} \qquad (36)$$

and

$$\frac{1}{\tau_p^2}(a^2 - 1 + 2ja) = \hat{A} \qquad (37)$$

which reduces to Haus' solution [2] when $a = 0$. The constraint $\mathrm{Re}\,\hat{A} < 0$ forces the "chirp" parameter a to be less than unity in magnitude.

$$a < 1. \qquad (38)$$

Separating η into real and imaginary parts yields

$$\eta = \eta_r + j\eta_i \qquad (39)$$

and solving (36) and (37) for the pulsewidth gives

$$\tau_p = 2\frac{QR}{\omega_0}\left(\frac{2(1-a^2)}{(R+1)^3(-\Gamma_{IO})(1 - G + 4\eta_r Y_0 G)}\right)^{1/2}. \qquad (40)$$

The pulse amplitude is

$$v_0 = \frac{QR}{2Y_0\omega_0\tau_p\alpha|\eta|}\left(\frac{3a}{\alpha I_{\mathrm{dc}}\eta_r\eta_i(R+1)^3\Gamma_{IO}}\right)^{1/2}. \qquad (41)$$

Note that according to (18), $\eta_i < 0$ and hence $\eta_i\Gamma_{IO} > 0$, so that real solutions result, provided $a > 0$. Thus, combining with (38),

$$0 < a < 1. \qquad (42)$$

The *FM* deviation of the pulse is a/τ_p where the "chirp parameter" a may be related to η using (36) and (34):

$$a = \frac{3(\eta_r^2 - \eta_i^2)}{4\eta_r\eta_i} + \sqrt{\left[\frac{3(\eta_r^2 - \eta_i^2)}{4\eta_r\eta_i}\right]^2 + 2}. \qquad (43)$$

Introducing (42) we find the condition

$$\alpha I_{\mathrm{dc}} > \frac{\sqrt{10} - 1}{3}\omega_0 C_j. \qquad (44)$$

Fig. 4 shows plots of P_p (average pulse power) and τ_p versus I_{dc}. There is another relationship between I_{dc} and P_p which is governed by the detector-voltage driver part of the circuit. By plotting these relationships on the same graph and looking for the intersections, points where the solutions are consistent can be determined. The intersections determine the system steady-state operating points.

An empirical formula for I_{dc} in terms of the average microwave power in the circuit is

$$I_{\mathrm{dc}} = I_{\mathrm{dc}O}(1 - kP_p) \qquad (45)$$

where

$$P_p = \langle |s_4|^2 \rangle. \qquad (46)$$

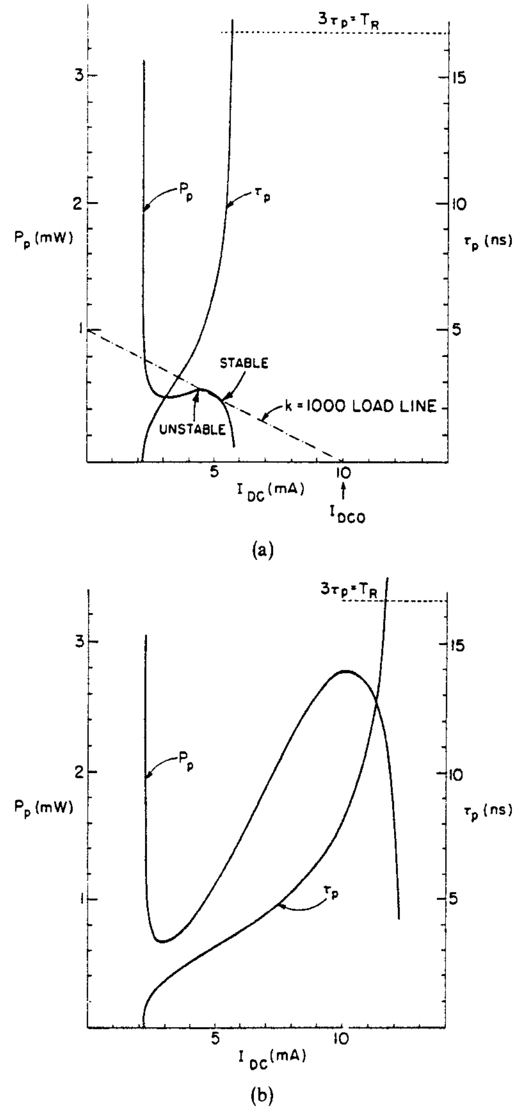

Fig. 4. Power P_p and pulsewidth τ_p versus dc bias current I_{dc}. (a) $G = 1.08$, load line drawn to correspond to values in Table I. (b) $G = 1.04$.

In the experimental system, k is adjustable from 10^{-2} to 10^4, while T_A is somewhere between 1.5×10^{-7} and 3×10^{-8} s. Fig. 4(a) indicates how a typical function from (43) intersects a computer-generated solution. Of the three intersections, only the one on the right is assumed physical. The argument that is used is that the intersection on the right and the one in the center seem to be in one-to-one correspondence with the laser model [2]. To relate the graphs in Fig. 4 with those of Haus [2], we may imagine a plot of P_p against I_{dcO} where I_{dcO} is an externally adjustable parameter. In the laser case, the intersection whose power increases with decreasing gain (bias) has been shown to be unstable. It is clear that raising the bias I_{dcO} will lead first to an intersection on the "stable" branch of the $P_p(I_{dc})$ curve. This intersection may not correspond to a physical solution because the system may be CW operating. But if the CW operation becomes unstable at some value of I_{dc} (as it must if mode locking is realizable), then the "stable" intersection point will be reached.

There is no correspondence between the left intersection and the solutions in the laser case. This may be attributable to the fact that the laser was analyzed with a simple gain and absorber model, whereas in the present analysis, reactive effects were included in both amplifier and absorber.

VI. Self-Starting Criterion

We have mentioned that the stability of isolated mode-locked pulses requires that the net gain between pulses be negative. If the net gain cannot adjust between the value required from the mode-locking solution and the small-signal value (in the absence of a signal), then the system cannot be self-starting. We shall now investigate the conditions for self-starting.

The concept of a self-starting mode-locked system involves two steps. First, a single mode of some number of half wavelengths within the waveguide resonator grows, resulting in a CW signal. The requirement for this is

$$G - 1 > 4\eta_r Y_0 G. \tag{47}$$

After the system is CW operating [$s(t)$ = constant independent of time], $s(t)$ may "buckle" into a pulse waveform. Such instability in CW operation is necessary if the system is to be self-starting.

We examine the stability of a small perturbation $a(T)e^{j\phi(T)}$ which travels through the system at some submultiple of the round-trip time T_R [5]. That is,

$$s = s_0 + \delta s = s_0 + a(T)e^{j\phi(T)} \exp\left(j\frac{2\pi mt}{T_R}\right) \tag{48}$$

where s_0 is real. The power is

$$\begin{aligned} P &= P_0 + \delta P + \delta P^* = |s|^2 \\ &= s_0^2 + a(T)s_0\left\{e^{j\phi(T)} \exp\left(j\frac{2\pi mt}{T_R}\right) + c.c.\right\}. \end{aligned} \tag{49}$$

When the system is operating CW, from (31), we have

$$(G - 1 - 4\eta_0 Y_0 G - j\psi) + (4Y_0\eta_0\alpha)^2\alpha I_{dc}^0|\eta_0|^2 P_0 = 0. \tag{50}$$

Since

$$\alpha I_{dc} \gg \omega_0 C_j \tag{51}$$

at the biases where (47) is satisfied, by using (18) we may approximate (50):

$$G - 1 - \frac{2Y_0 G}{\alpha I_{dc}^0} + Y_0^2 \frac{P_0}{\alpha(I_{dc}^0)^3} = 0. \tag{52}$$

This is the gain in one transit time which is zero in the steady state. To find the growth rate of a perturbation, we ask for the gain perturbation, we must write I_{dc} in terms of δs. Obviously I_{dc} is not, any more, a direct current but has time dependence. Instead of (45), we write

$$I_{dc} = I_{dcO}\left[\delta(\omega) - \frac{k\delta P}{1 + j\omega T_A}\right] \tag{53}$$

where T_A is the time constant of the detector and voltage-driver circuit and

$$T_A \gg T_R. \quad (54)$$

This is equivalent to saying that the biasing loop averages over many pulses. Examining only positive frequencies, we write

$$\delta I_{dc} \cong -kI_{dcO} s_0 \frac{a(t)e^{j\phi(T)}}{1 + j\dfrac{2\pi m T_A}{T_R}}. \quad (55)$$

Strictly speaking, we would have to treat ω in (53) as a variable, including the growth rate of the perturbation. But this growth rate, in general, will be small compared with $2\pi m(T_A/T_R)$ and hence can be ignored. If the perturbation is included, (52) becomes

$$\frac{Y_0 P_0}{\alpha (I_{dc}^0)^2}\left[\left(2G - \frac{3Y_0 P_0}{(I_{dc}^0)^2}\right)\delta I_{dc} + \frac{Y_0}{(I_{dc}^0)}\delta P\right] = s_0 T_R \frac{\partial}{\partial T}\delta s. \quad (56)$$

For the system to be self-starting we would like $a(T)$ to grow. Expressing δP and δI_{dc} in terms of $a(T)$, by using (49) and (55), we find

$$\left[\left(\frac{3Y_0 P_0}{I_{dcO}(1 - kP_0)^2} - 2G\right)\left(\frac{kI_{dcO} T_R^2}{T_R^2 + (2mT_A)^2}\right) + \frac{Y_0}{I_{dcO}(1 - kP_0)}\right] > 0. \quad (57)$$

Using typical numbers from Table I in (52) and (57), we obtain

$$T_A/T_R > \sqrt{k}/60. \quad (58)$$

Unless k is very large, this provides a very mild limitation on T_A because we have assumed $T_A/T_R \gg 1$.

VII. Relaxation Oscillations

The analysis of relaxation oscillations is similar to that for self-starting. However, in this case we cannot assume that the frequency of the relaxation oscillation is near $2\pi m/T_R$. Equation (56) still holds, but now we have to take (53) with $j\omega$ not preset. We obtain

$$\left\{\frac{2Y_0 P_0}{\alpha (I_{dc}^0)^2}\left[\left(\frac{3Y_0 P_0}{(I_{dc}^0)^2} - 2G\right)kI_{dcO} + \frac{Y_0}{I_{dc}^0}(1 + j\omega T_A)\right] - j\omega T_R(1 + j\omega T_A)\right\}\delta P(\omega) = 0. \quad (59)$$

For stability we would like roots of ω in the lower half ω plane.

$$(j\omega)^2 + \left[\frac{1}{T_A} - \frac{2Y_0^2 P_0}{\alpha T_R I_{dcO}^3(1 - kP_0)^3}\right]j\omega + \left[\frac{-2Y_0 P_0}{T_A T_R \alpha I_{dcO}^2(1 - kP_0)^2}\left\{\frac{3Y_0 P_0 k}{I_{dcO}(1 - kP_0)^2} - 2GkI_{dcO} + \frac{Y_0}{I_{dcO}(1 - kP_0)}\right\}\right] = 0. \quad (60)$$

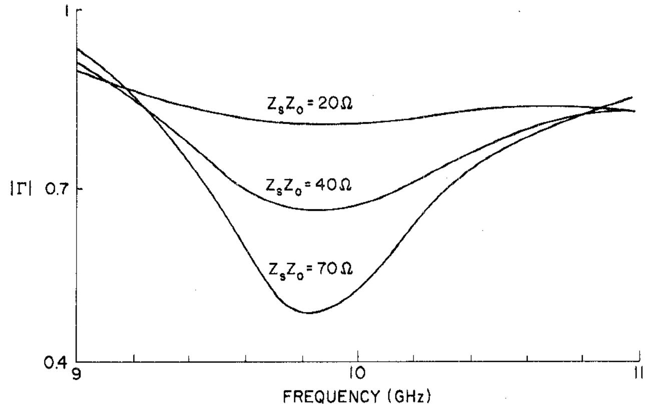

Fig. 5. Calculated reflection coefficient of Schottky diode and embedding circuit versus bias current.

TABLE I

Y_O	.01 mho
P_O	0.5 mW
I_{DCO}	10 mA
α	40 V^{-1}
kP_O	.5
T_R	50 ns
R	- 1/3
ω_O	$2\pi \times 10^{10}$
C_j	1 pF
Q	40

The system will be stable when

$$\frac{3Y_0 P_0 k}{I_{dcO}(1 - kP_0)^2} - 2GkI_{dcO} + \frac{Y_0}{I_{dcO}(1 - kP_0)} < 0 \quad (61)$$

and

$$\frac{T_R}{T_A} > \frac{2Y_0^2 P_0}{\alpha I_{dcO}^3(1 - kP_0)^3}. \quad (62)$$

With the values listed in Table I used, the second expression means, that for a microwave mode-locked system to be stable

$$T_A < 50T_R \approx 2.5\ \mu s. \quad (63)$$

VIII. Experiment

The IMPATT diode amplifier was designed and built by Weng C. Chew and is described in his thesis [6]. It had a 150–300-MHz useful bandwidth, depending on the bias. The microstrip circuit for the Schottky barrier diode was fabricated on a 30-mil *TFE* substrate. A plot of the calculated magnitude of the reflection coefficient [7] as a function of bias is shown in Fig. 5. The circuit was designed to tune out the susceptance produced by C_j.

A great deal of flexibility was built into the experimental system. The four parameters that could be adjusted were G,

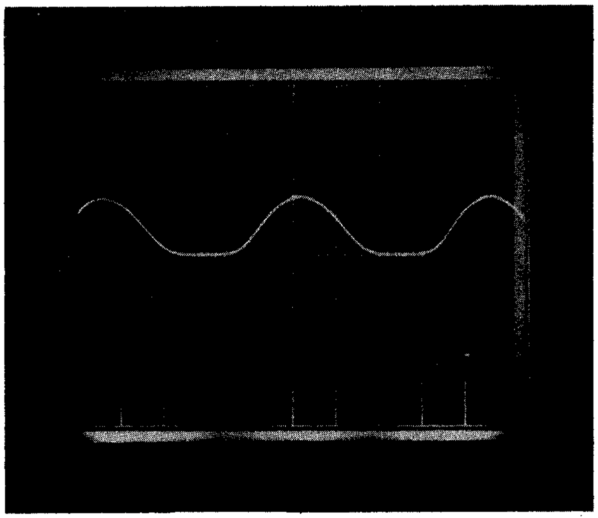

(a)

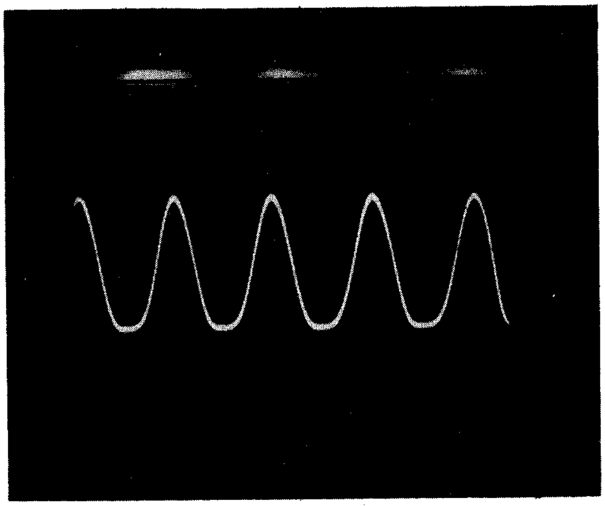

(b)

Fig. 6. Observed pulse shapes. (a) Long system with 1 pulse per round-trip time (10 ns/div). (b) Long system with 2 pulses per round-trip time (10 ns/div).

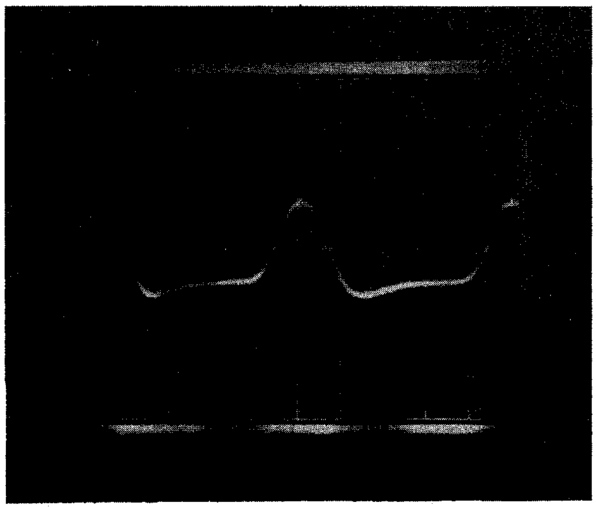

(a)

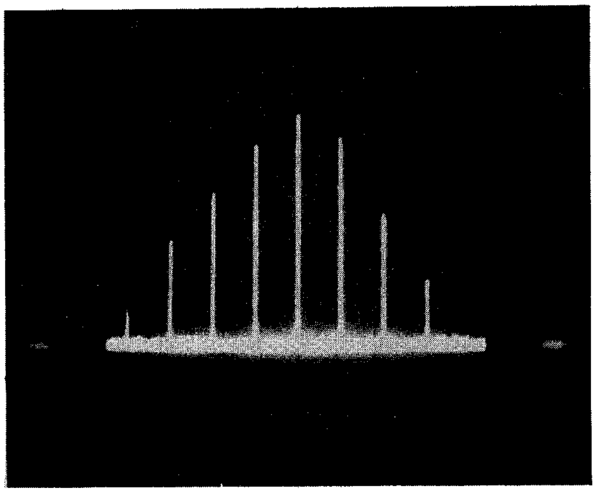

(b)

Fig. 7. (a) Short system at 5 ns/div. The distortion caused by limitations in the detector bandwidth. (b) Log amplitude of the spectrum of the pulse shown in 6(a). Horizontal: 20 MHz/div; vertical: 10 dB/div.

I_{dcO}, k, and the bias on the IMPATT that affects both G and the parameters in (13). Typical values of the rest of the parameters are listed in Table I.

The first system that was built had $T_R \approx 50$ ns. It operated either with one or two pulses per round-trip time (see Fig. 6). The pulse lengths were between 5 and 15 ns. The system mode locked over an 8-dB variation in G_L. The locking range for I_{dc} was in agreement with theoretical prediction.

The waveguide was shortened so that $T_R \approx 25$ ns. Only one pulse per round trip was observed with this system. Pulse lengths as short as 4 ns were achieved. The average pulse power was between 1 and 10 mW. For some biases there were in the system as much as 10-dB extra gain that had to be reduced by an attenuator. The system seemed relatively insensitive to the k of (45).

Fig. 6(a) is a time-domain picture of the pulse shown in Fig. 7(b). Fig. 7(b) is a photograph of the pulse spectrum over a 70-dB range. Notice the linear falloff of the tails, which supports the sech (t/τ_p) dependence near the pulse center. The Fourier transform of

$$s(t) = \text{sech } (t/\tau_p) \tag{64}$$

is

$$S(\omega) = \pi \text{ sech } (\pi \tau_p \omega/2). \tag{65}$$

Taking the log of $S(\omega)$ near one of the tails, we have

$$20 \log_{10} S(f) = 20 \log_{10} \pi - 20(\pi^2 f \tau_p) \log_{10} e. \tag{66}$$

From Fig. 7(b) we can obtain a $\tau_p = 6.8$ ns pulsewidth that agrees with the oscilloscope display in Fig. 6(a).

Forced mode locking [8] was also attempted with the short system and was successful. The forcing signal was applied to the Schottky barrier diode. Various combinations of forced and passive mode locking were also tried. A locking phenomenon similar to that seen in injection locking was observed in that, over a certain range of modulation frequencies, the pulse repetition period could be controlled

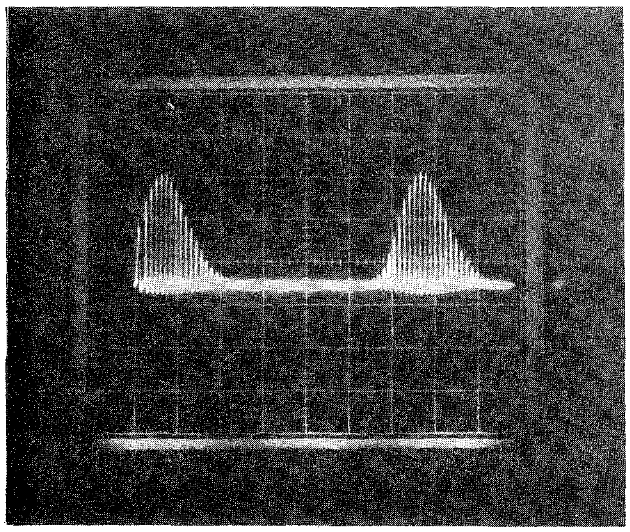

(a)

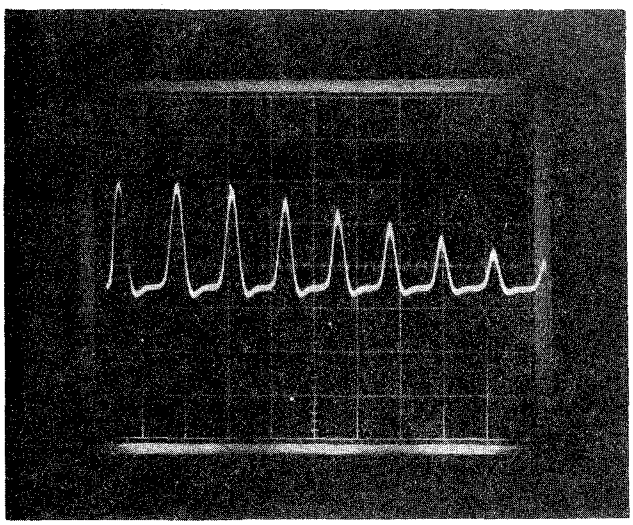

(b)

Fig. 8. (a) Relaxation oscillations in the short system (0.2 μs/div). (b) Same as (a), except 20 ns/div.

by the applied modulation frequency. No difference was found in pulse length.

By adjusting the time constant T_A, relaxation oscillations could be obtained or suppressed for either the passive or the passive combined with forced mode-locking cases (see Fig. 8). Relaxation oscillations could also be obtained in the absence of mode locking.

IX. Discussion

The present experiments are preliminary in that they open up several avenues for further investigation.

1) The mode locking principle applied to high-power devices at S or X band may give pulse powers and pulsewidths of interest for radar applications. With such an application in mind, power maximization is a topic for further investigation.

2) Scaling of the system to higher frequencies can give very much shorter pulses because the pulsewidth is primarily determined by the *net* system bandwidth. At millimeter wavelengths, a fully integrated mode-locking system offers an attractive method for short pulse generation.

3) The parameters of the microwave system may be adjusted and measured more conveniently than those of an optical mode-locking system. The pulsewidth and shape measurements are also performed more conveniently at microwave frequencies than at optical frequencies. Experimental studies of the microwave system may provide guidance for the design of optical systems.

References

[1] C. C. Cutler, "The regenerative pulse generator," *Proc. IRE*, vol. 43, pp. 140–148, Jan. 1955.
[2] H. A. Haus, "Theory of mode locking with a fast saturable absorber," *J. Appl. Phys.*, vol. 46, pp. 3049–3058, 1975.
[3] A. A. M. Saleh, *Theory of Resistive Mixers*, Res. Monograph No. 64. Cambridge, MA: MIT Press, 1971.
[4] H. A. Haus, "Passive FM mode locking with a nonlinear refractive index medium," RLE Progress Report No. 115, Research Laboratory of Electronics, Cambridge, MA: MIT, Jan. 1975.
[5] ——, "Parameter ranges for CW passive mode locking," *IEEE J. Quantum Electron.*, vol. QE-12, pp. 169–176, 1976.
[6] W. C. Chew, "Broadbanding of IMPATT diode reflection amplifier on microstrip," S.B. thesis, MIT, Cambridge, MA, 1976.
[7] P. Penfield, Jr., *MARTHA User's Manual*. Cambridge, MA: MIT Press, 1971.
[8] H. A. Haus, "A theory of forced mode locking," *IEEE J. Quantum Electron.*, vol. QE-11, pp. 323–330, 1975.